THE UNIVERSITY OF
MELBOURNE

$U(1) \otimes U(1)$ Gauge Fields on Domain Walls

Damien George
Supervisor: Prof. Raymond Volkas

Part IV honours thesis
November 2004

Abstract

We begin by giving an overview of the historical development and the mathematical preliminaries for the domain wall, or brane world model. Included is an exposition of a simple Lagrangian which permits a domain wall configuration and an example of a warped gravitational metric. We then proceed to develop a technique for analysing the stability of static solutions to a set of field equations, motivated by the necessity to prove stability of gauge fields semi-localised to a domain wall. The technique is based on finding the eigenvalues associated with normal modes of small perturbations upon a static solution. We outline a successful implementation of this technique on a variety of domain wall models, including a $U(1) \otimes U(1)$ model as previously studied by Rozowsky et al. [1]. In addition to this perturbative eigenvalue analysis, we also numerically time evolve the field equations of motion to obtain a more intuitive understanding of their stability behaviour. Our main results are establishing the stability, for a large range of parameters, of both the scalar and gauge field static solutions in the $U(1) \otimes U(1)$ case. Finally, we introduce gravity into the action integral in a way which generalises the Randall-Sundrum model [2, 3] and includes $U(1) \otimes U(1)$ gauge fields. While we obtain the standard domain wall solutions, we show there are no finite static solutions for localised or even semi-localised gauge fields.

Signature .....

Statement of contributions

The introduction and mathematical overview in Sections 1 and 2 are original expressions of my own understanding and knowledge of the subject at hand. I independently developed and implemented the perturbative stability techniques described in Section 3, along with the time evolution algorithm. I have carried through the derivation of all the equations of motion, as obtained from the action integrals. My supervisor and others have previously used the $U(1) \otimes U(1)$ and gravitational Lagrangian but the equations given in this thesis have been re-derived. The numerical techniques given in Appendix A are widely known and used, but I have given my own derivation and a description of my understanding. I have generated all the plots and figures, both 2D and 3D, many with the help of Gnuplot. I have written all the code used to obtain the results presented except the `tqli` tri-diagonal matrix solver from Numerical Recipes in C.

1 Introduction

There is no doubt as to the success of the standard model of particle physics in experimental prediction. This model is expressed in the language of quantum field theory, a quantised form of classical field theory. In classical field theory, all forms of matter (fermions) and force carrying particles (bosons) are represented by universal functions, one for each distinct type of particle. A field can be real or complex and the simplest form, a scalar field, has a single component. Other forms include spinors which describe fermions and tensors which describe bosons, with the number of components directly related to the polarisation degrees of freedom.

The content of a field theory, the fields and their interactions, is conveniently summarised by the integral of a Lagrangian, known as the action. Finding a stationary point of the action with respect to a field yields the Euler-Lagrange equation of motion for that field. This is similar to Fermat's principle which states that light must follow the path of least time, from which Snell's law can be derived. In classical mechanics, the Lagrangian is the kinetic energy minus the potential energy and can be related to the Hamiltonian. In field theory, a similar approach is taken and the choice of terms in the Lagrangian, somewhat an art, is where most of the physics lies. The rest of the work goes into finding solutions to the equations of motion for particular scenarios, for example cross sections and the expansion of the universe.

The most fruitful aid for deciding what terms to include in a Lagrangian is the idea of a symmetry – a transformation which changes one thing but not another. In the case of a physical theory, we look for symmetries which change the fields but leave the Lagrangian invariant. Generally, the thing that changes due to the symmetry transformation is not physically measurable, so if two Lagrangians are equivalent under some symmetry, then they describe the same physics. This is the motivation behind almost all of the theories in use today.

Symmetries of a Lagrangian can be broadly classified into two categories, global and local, and by Noether's theorem there exist corresponding conservation laws. A symmetry is global when the field which is being transformed is modified in exactly the same way at all locations in space-time. An example would be changing the phase of an electron wave function by the same constant angle at each location in space. Since we are only able to measure relative phase differences, this change does not affect the physics we observe; consequently we measure conservation of electric charge. A global phase transformation is a continuous symmetry because the phase can be any real number. Discrete global symmetries also exist in certain Lagrangians, for example parity, charge conjugation and time reversal.

Local symmetries are associated with much richer physics than global ones, since local transformations act on a field differently at each point in space-time. As a consequence, terms involving the derivative of the transformation are present in the Lagrangian and it is no longer trivially invariant. To restore the invariance, a new field is added to the theory which transforms in just the right way; it brings in a term which cancels the unwanted derivative term. This new field is called a gauge field, which stems from the physical idea that two independent observers do not need to calibrate their wave function measuring device. So long as they both measure the wave function in the same way relative to its associated gauge field, they will agree on their observations. A gauge field

carries a calibration independent measurement from one place to another.

This idea of adding new fields to restore an initially non-existent symmetry may seem unjustified at first, but it has been used to succinctly describe all the known force carrying particles. A specific gauge symmetry is named by the group of transformations which keep the Lagrangian invariant. For a concrete example, consider electromagnetism where the electron and positron are the fermions associated with a certain four dimensional Dirac spinor[1]. The local symmetry is just a local phase rotation of the spinor and is denoted by $U(1)$, the group of one dimensional unitary transformations. The gauge field, or gauge boson, associated with this local symmetry is identified with the photon[2] which mediates the electric force between charged particles.

Quantum electrodynamics (QED) is a $U(1)$ Abelian gauge theory which has been quantised by certain commutator and anti-commutator relations. By finding the extrema of the action derived from the QED Lagrangian, one arrives at both Maxwell's equations and the Dirac equation, which is a relativistic generalisation of the Schrödinger equation. The standard model Lagrangian uses the same ideas as QED; it is an $SU(3)\otimes SU(2)\otimes U(1)$ gauge theory and describes electromagnetism, the weak and strong forces, the leptons and the quarks. This theory has had fantastic success in explaining all of the accepted experimental data. Despite this, many phenomena, including neutrino mass, dark matter and energy and gravity, are explained poorly or not at all. Furthermore, the standard model requires experimental input for its nineteen free parameters, not including neutrino masses. Proposed extensions to the model are abundant, with much recent focus on so-called "brane world" models that require the existence of one or more extra spatial dimensions.

Going back to more fundamental issues, it is interesting to consider how many spatial dimensions a physical theory could be expressed in, while still giving consistent predictions to our current observations of the universe. Our everyday experiences convince us that our position and momentum are confined to three spatial dimensions and one time dimension. Indeed, the success of special and general relativity, formulated in $3+1$ dimensions, is a big hint that extra dimensions are not required. Disregarding these considerations, Kaluza [4] reformulated general relativity in $4+1$ dimensions and showed that Maxwell's equations arose naturally if one identified some of the extra components of the metric tensor with the four-potential of electromagnetism. In Kaluza's work, it was proposed that we only measure variations of the fields (the gravitational metric and four-potential) in the conventional $3+1$ dimensions. Dependence on the new dimension was suppressed in order to agree with experiment.

The physical reality of such an extra dimension was not entertained until the work of Klein [5] established the plausibility of an extra Kaluza dimension if it was small, perhaps of order the Planck length, and circular in topology. The ordinary matter which we experience is the zeroth mode of excitation in this circular dimension and because it is so small, the higher order modes require large amounts of energy and we have not measured them. The realisation that including small extra dimensions did not immediately invalidate a theory led

[1] A four dimensional spinor gives four degree of polarisation freedom; two for electron spin up and down and two for positron spin up and down.

[2] The photon field is a four dimensional, rank one tensor (just a four-vector), and as such has four polarisation states. Two of them are the physically observable polarisations of light. The other two cancel due to the masslessness of the photon.

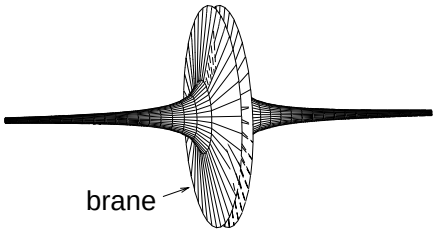

Figure 1: Visualisation of two spatial dimensions exponentially suppressed in a large extra dimension. The centre of the figure is called the brane; it is where standard model matter can propagate freely. Off the brane is known as the bulk; since gravity has only one degree of freedom here, transverse to the brane, we observe the familiar $1/r^2$ law for gravity.

to radical proposals for extensions to the standard model; this line of thought brought about string theory which proposes six or seven tiny extra dimensions.

In the mean time, $3+1$ dimensional special relativity had huge success in describing the underlying space-time of the standard model. If there existed extra dimensions not accounted for in the standard model, then energy and momentum would constantly go missing in the particle collider experiments. This firmly established belief, that if extra dimensions exist they must be tiny, has been overthrown by the recent work of Arkani-Hamed, Dimopoulos and Dvali [6, 7, 8]. In their model, the ADD model, they allow the size of extra circular dimensions to be much larger by assuming that the standard model matter is somehow confined to a specific $3+1$ dimensional location, called the brane; the rest of space is called the bulk. This is a more restricted version of Kaluza's requirement that dependence on the extra dimension should be suppressed. The ADD model agrees trivially with the observed decay rates and scattering cross sections because it is equivalent, at low enough energies, to the standard model. It might seem that extra dimensions are a trivial addition if everything is confined to the brane, but the bulk must also be counted in general relativity calculations since space-time is described by gravity. The restrictions on the size of the large extra dimensions now come from gravitational experiments; they must still be quite small, of order 1 millimetre, just not as small as in Kaluza-Klein theories.

Much work has spawned from the ADD model, most notable is that of Randall and Sundrum [2, 3], who allowed the gravitational metric to explicitly vary in the extra dimension. They showed that a certain form of the metric lead to warping, or exponential suppression, of the conventional $3+1$ dimensions away from the brane, leaving space-time restricted to a single dimension in the bulk; see Figure 1. This idea eliminates the need for the bulk to have a circular topology – the extra dimension can now be infinite! Our ideas about extra dimensions have progressed from none at all, because we can't see any; through tiny ones, that we haven't seen yet; to an infinite bulk, that only gravity can see. An assumption underlying the RS model is the Anti-de Sitter[3] nature of the bulk space-time. In fact, the regions to the left and right in Figure 1 must

[3]An Anti-de Sitter space has constant negative curvature, abbreviated as AdS_n, where n is the number of dimensions. An approximate AdS_n space has almost constant negative curvature.

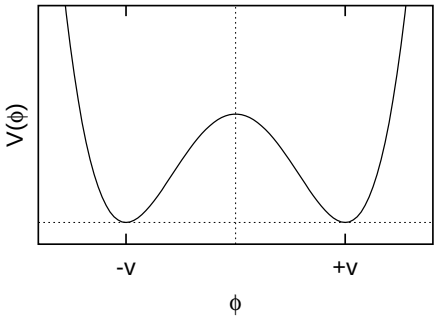

Figure 2: The simplest kind of scalar potential with degenerate minima; one at $\phi = v$, the other at $\phi = -v$. It can be used to support a background scalar field for an RS-like warped space-time.

be *different* AdS_3 spaces in order to support a stable brane at the centre. It was later realised that this seemingly artificial patching of space-time could be made to occur much more naturally by the coupling of gravity to dynamically created domain walls; see for example [9, 10].

As in the ferromagnetic case, a domain wall is the relatively thin area that separates two opposing regions. In the field theory scenario, the value of a background scalar field takes the place of the magnetic moment. It is possible to encourage the scalar field to take specific values by putting it in a "potential"; akin to magnetic alignment, the potential being minimised by certain values of the scalar field. A magnetic domain wall arises because magnets all pointing up is a ground state just as is magnets all pointing down[4]. The simplest potential that can give similar behaviour for scalar fields is shown in Figure 2. The two degenerate minima of $V(\phi)$ give possible values for the scalar field to asymptote to, a domain wall being created when it takes opposite minima in the left and right regions of the bulk.

By simply combining gravity with the usual scalar field and a suitable potential, a domain wall solution arises which is compatible with the warped gravitational metric in the RS model. This gives the basis of an elegant model with one or more infinite extra dimensions that agrees with our current observations of both gravity and standard model phenomena. In addition, the scalar fields associated with these brane world models may be related to the undiscovered Higgs scalar field. Furthermore, as was the initial motivation for the RS model, an extra large dimension in which gravity can propagate gives a neat solution to the hierarchy problem. We measure gravity to be much weaker than the other forces because it is diluted by the volume of the bulk.

The major theoretical obstacle in this line of work is providing a mechanism to localise standard model matter to the brane. There has been some progress in this area for fermions; Ringeval et al. [9] have shown that a generalisation of the Dirac Lagrangian permits bound fermionic states with a discrete mass spectrum. Furthermore, the confinement lifetime of these particles is shown be longer than the age of the universe. Unfortunately, these mechanisms do not

[4]To clarify, the magnet is not in an external field, the different ground states coming from the relative potentials between individual magnets. Similarly, the scalar field must be given some potential to give it a reason to have a particular value.

carry over to the the gauge field case and while there are some proposals, for example [11], there are problems with charge universality as discussed in [12].

The problem of localising gauge fields to a domain wall must be solved to realise a full brane world model. In a step towards this goal, Rozowsky, Volkas and Wali [1] have studied a model with two background scalar fields in flat space-time, i.e. without gravity. They have found consistent solutions to the field equations of motion with two $U(1)$ style Abelian gauge fields semi-localised to the domain wall. Each field is strongly coupled to its associated scalar field and indirectly coupled, via the scalar potential, to the other scalar field and its gauge field. The semi-localisation comes about from the Meisner-like suppression of the gauge fields on one side of the wall and linear growth on the other side. This model may provide the beginnings of massless Abelian gauge field localisation with gravity.

In the work of this thesis, we investigate the dynamical stability of the scalar and semi-localised gauge field solutions in the Rozowsky et al. $U(1) \otimes U(1)$ model. Stability is a necessary condition for a brane world model, as the background fields must not be susceptible to decay from, for example, fluctuations in fermionic standard model wave functions. The technique that we develop for stability analysis is verified on domain wall models that are known to be stable or unstable from analytic topological arguments. Following this analysis, the $U(1) \otimes U(1)$ model is extended by including gravity in the action and we study the permissible solutions for the gauge fields.

A more technical overview of the brane world model and the RS warped gravitational metric idea is given in Section 2. We then begin our work in Section 3 with the development of techniques to analyse the field equations of motion, partially analytically and partially numerically. Sections 4, 5 and 6 apply these techniques to simple scenarios with both stable and unstable domain walls. This verifies the stability analysis procedure and allows us to gain some intuition as to what attributes a stable brane must have by studying time sequences of a perturbation. Section 7 establishes the stability of the scalar and gauge fields in the Rozowsky et al. model. We study the inclusion of gravity in this model in Section 8 and show, unfortunately, that the gauge fields are then fully suppressed both on and off the brane – there is no static localisation. We draw our conclusions in Section 9. Appendix A establishes the necessary numerical algorithms for stability analysis and finding solutions to differential equations. These techniques are used extensively throughout the work that follows.

2 Brane world basics

As discussed previously, it is possible to have large extra dimensions in a theory and the brane world model is a promising realisation of this idea. The underlying structure of this model is the domain wall, which sets up a background scalar field that restricts ordinary matter to an effective four dimensional space-time. Gravity is necessarily coupled to the domain wall and the two types of fields must have consistent solutions. The space-time metric must also be warped in such a way that we measure the familiar, weak, four dimensional gravitational attraction. In the following subsections, we give a more technical overview of the concepts of domain walls and warped gravitational metrics

2.1 Domain wall overview

A field theory is commonly described by an action, S, which is the integral of a Lagrangian density, $\mathcal{L}$. The action has units of energy by time and for a three space plus one time dimensional theory, the integral is over a four-volume

$$S = \int \mathcal{L}\left(\phi_i, \partial_\mu \phi_i\right)\ d^4x,$$

where the index μ runs over the four dimensions. The Lagrangian density is a function of all the fields in the particular theory, ϕ_i, and their first derivative, $\partial_\mu \phi_i$. There are terms for kinetic energy, mass, potentials and the interactions between fields. Each term should be Lorentz invariant in order for the theory to also describe special relativity. The Principle of Least Action states that the values of the fields must be such that the action is stationary with respect to an arbitrary change in each field. To apply this principle and obtain the equations of motion, each field is varied slightly and the resultant variation in the action set to zero. This gives the Euler-Lagrange equation

$$\frac{\partial \mathcal{L}}{\partial \phi_i} - \partial_\mu \frac{\partial \mathcal{L}}{\partial(\partial_\mu \phi_i)} = 0. \tag{1}$$

The Hamiltonian density can be derived from the Lagrangian density by subtracting the conjugate momenta, as in classical mechanics. The total energy of a system described by an action, the Hamiltonian, is the integral over all space of the Hamiltonian density

$$E = H = \int \left(\sum_i \left(\frac{\partial \mathcal{L}}{\partial(\partial_t \phi_i)}\, \partial_t \phi_i \right) - \mathcal{L} \right) d^3x. \tag{2}$$

The physics comes in choosing the terms in the Lagrangian[5], which is the kinetic energy less the potential energy. For the case of a single, real valued scalar field ϕ, the kinetic energy is the square of the first derivative. This choice is made as it yields a Klein-Gordon like equation of motion, with linear second derivatives of the field. We subtract the potential energy of the scalar field, $V(\phi)$, from the kinetic energy to get the Lagrangian

$$\mathcal{L} = \partial^\mu \phi\, \partial_\mu \phi - V(\phi). \tag{3}$$

For there to exist domain wall solutions, we choose the potential as shown in Figure 2 which has two degenerate minima at $\phi = \pm v$. This is the simplest potential for the desired domain wall behaviour and has the quartic form

$$V(\phi) = \lambda(\phi^2 - v^2)^2, \tag{4}$$

where λ and v are positive constants. Applying the Euler-Lagrange equation (1) to the Lagrangian (3) with the quartic potential, gives the equation of motion for the field ϕ

$$\partial^\mu \partial_\mu \phi + 2\lambda\phi\left(\phi^2 - v^2\right) = 0.$$

[5]The classical mechanics Lagrangian is the integral over all space of the density, $L = \int \mathcal{L}\ d^3x$. To keep the language simpler, Lagrangian will henceforth be taken to mean Lagrangian density.

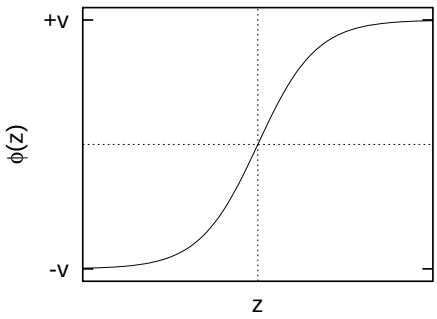

Figure 3: The archetypal domain wall, or kink, solution. This real scalar field asymptotes to $\pm v$, the minima of the quartic potential. Note that the negative of this solution is also a solution. Similarly, any translation is a solution because the equation of motion (ultimately the Lagrangian) is translationally invariant.

and the associated energy, using (2), is

$$E = \int \left((\partial_t \phi)^2 + (\nabla \phi)^2 + V(\phi) \right) d^3x.$$

A domain wall solution, also known as a kink, must not vary with time in order to give a constant background field. We look for solutions that depend only on the z degree of freedom, which we interpret as the extra dimension. A slice of x–y plane then becomes a two dimensional space with a uniform scalar field value. We also require the kink to have finite energy[6] as defined by (2.1) which means that the integrand must fall to zero faster than $1/z$ as $z \to \pm\infty$. Since the terms in the integrand are non-negative, it must be that ϕ approaches a constant and $V(\phi)$ approaches zero. The second condition requires $\phi \to \pm v$ which immediately satisfies the first condition. The straight lines, $\phi = \pm v$, are obviously solutions to (2.1), but we desire something a little less trivial. By demanding different boundary conditions for the kink on the left and the right we find the solution

$$\phi(z) = v \tanh\left(\sqrt{\lambda}\, v z\right), \tag{5}$$

which is shown in Figure 3. In fact this is the only non-constant solution to equation (2.1), up to a reflection or translation in the z direction. To see this, note that if ϕ is asymptoting to v from above then the second derivative with respect to z must be positive and so ϕ must be curved upwards. If it is above v and curved up, ϕ can never go below v and so must always curve up, never being able to reach v or $-v$ at the other boundary. A similar conclusion is reached if ϕ is asymptoting to $-v$ from below. Thus it must be that ϕ is bounded between $\pm v$ and the solution is then given by (5).

A background scalar field must be stable, with respect to time, in order for it to provide a domain wall on which the standard model can be reproduced. If it were not stable, any small fluctuation in a field on the wall would disturb the brane and it would collapse. Proof of stability is therefore just as necessary as existence of solutions in the brane world model and of course in many other

[6]Domain walls are sometimes referred to as solitonic solutions because they have finite and localised energy.

situations. The kink described by (5) can be shown to be stable by a topological argument which we outline here. First of all the scalar potential must have multiple distinct global minima and a solution should continuously interpolate between *different* minima. Since the kink has finite energy initially and energy is conserved, every instant of a time evolved solution must also have finite energy. If the asymptotic behaviour of the kink were to change as time developed, then this finite energy condition would be violated. Thus ϕ remains constant at $z = \pm\infty$ and a time dependent solution will always interpolate between its original *discrete* global minima. The stability of the kink is then guaranteed by the uniqueness of a solution with given boundary conditions. See Chapter 2 of Rajaraman [14] for a more in-depth argument of topological stability.

The important criterion for this kind of stability is the existence of disconnected minima, in order that the scalar field be bound asymptotically to specific regions for all time. In this thesis, we are concerned with stability in cases which are not as obvious as those simply requiring disconnected global minima. Specifically, with the inclusion of gauge fields, there is no known general proof for topological stability. The method that we later employ requires temporal analysis of perturbations upon a given static solution.

2.2 Warped metric overview

The nature of space-time is described by Einstein's field equation for the gravitational metric, $g_{\mu\nu}$, where the indices run over the number of dimensions. Throughout this thesis, Greek indices are used in four dimensions, capital Latin letters in five dimensions. Measurement in space-time is achieved using the metric equation

$$\mathrm{d}s^2 = g_{\mu\nu}\mathrm{d}x^\mu \mathrm{d}x^\nu,$$

where $\mathrm{d}s^2$ is the measure distance and $\mathrm{d}x^\mu$ are the coordinate distances. In flat space-time the metric becomes diagonal and constant with the pseudo-Euclidean form

$$\mathrm{d}s^2 = \mathrm{d}t^2 - \mathrm{d}x^2 - \mathrm{d}y^2 - \mathrm{d}z^2.$$

To include gravity in a theory, the flat space metric $\eta_{\mu\nu}$ changes to $g_{\mu\nu}$ and the existing fields become minimally coupled to gravity. The Ricci scalar, R, is added to the Lagrangian and the whole thing is multiplied by $\sqrt{|g|}$ where g is the determinant of the metric. Then by varying the fields and keeping the action stationary (as before but now the gravitational metric contributes up to ten new fields) Einstein's equations are reproduced. In the five dimensional case they are

$$G_{AB} = R_{AB} - \tfrac{1}{2}g_{AB}R = \tfrac{1}{2\kappa}T_{AB}, \tag{6}$$

where the G_{AB} is the Einstein tensor, R_{AB} is the Ricci tensor related to the Ricci scalar as $R = g^{AB}R_{AB}$, T_{AB} is the stress energy tensor and the gravitational proportionality constant is $\kappa = 1/16\pi G$.

The Randall-Sundrum model was motivated by the possibility that gravity could be confined to a domain wall, even if there was a very large extra dimension for the fields to propagate in. This turned out to be a fruitful idea and was originally shown by artificially putting in a non-dynamical domain wall. This amounts to specifying the stress energy tensor and once this is done, Einstein's equations can be used to solve for the gravitational metric. Randall and

Sundrum showed [2, 3] that for an infinitely thin domain wall, there exists a consistent solution for the gravitational metric which confines "gravitons" to the domain wall. Their solution was of the form

$$\mathrm{d}s^2 = \mathrm{e}^{-|w|}(\mathrm{d}t^2 - \mathrm{d}x^2 - \mathrm{d}y^2 - \mathrm{d}z^2) - \mathrm{d}w^2,$$

where w is the extra dimension. It can be seen that on the brane, $w = 0$, distances are measured just as in the flat space case. However, for any moderate distance from the brane, the exponential dies off very quickly and the space looks one dimensional. This is depicted, in lower dimensions, in Figure 1.

The initial brane that was put in by hand had the form of a delta function, which allows for an analytic solution but at the price of a cuspy $-|w|$ term. A more elegant way to achieve an equivalent warping of the metric, without putting a brane in by hand, was discovered later on, see for example [9, 10]. Quite simply, we build on the Lagrangian defined by (3) and include gravity to get an action of the form

$$S = \int \left(\kappa R + g^{AB}\partial_A\phi\,\partial_B\phi - V(\phi)\right)\sqrt{g}\; d^5x, \tag{7}$$

where the potential is the previously used quartic (4) and the metric signature is $(+,-,-,-,-)$. The metric ansatz we employ is equivalent to that in the RS model

$$\mathrm{d}s^2 = \mathrm{e}^{f(w)}(\mathrm{d}t^2 - \mathrm{d}x^2 - \mathrm{d}y^2 - \mathrm{d}z^2) - \mathrm{d}w^2,$$

where $f(w)$ is an arbitrary function to solve for and will determine the exact shape of the warped metric. We look for solutions that depend only on w and denote the corresponding derivative by prime. We can compute G_{AB} and T_{AB} from the action (7) and then use Einstein's equations (6) to get the equation of motion for f. We also vary ϕ in the action to get its corresponding Klein-Gordon equation

$$\begin{aligned} f'' &= \tfrac{-2}{3\kappa}\phi'^2, \\ \phi'' &= -2f'\phi' + 2\lambda\phi\left(\phi^2 - v^2\right). \end{aligned}$$

Asymptotic analysis gives constraints on some of the parameters and then these equations are solved numerically, see Appendix A.2 for details of the general method. Figure 4 shows the results with ϕ looking almost identical to that depicted in Figure 3. This domain wall is coupled to gravity to give warping which is qualitatively equivalent to the RS model, the main difference being the smoothed out metric function f.

By simply solving for the metric and the domain wall in a coupled set of field equations, we obtain both a dynamically generated brane and a warped geometry which confines gravity to three space dimensions. A similar technique is used in a later section with two scalar fields and two gauge fields.

3 Perturbative stability analysis

In this section we outline the techniques used to analyse the behaviour of static solutions under a small perturbation. To this end, we must first obtain the static solutions themselves – analytically if possible, but in general numerically.

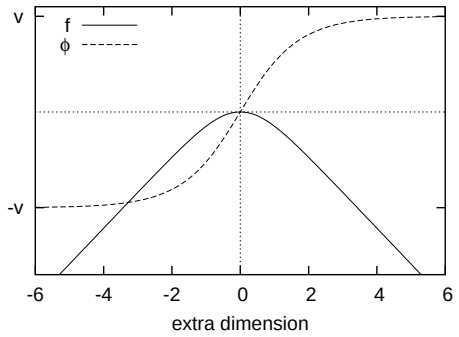

Figure 4: Solutions for the gravitational warp factor f and the domain wall ϕ. Since f is negative in the bulk, the metric looks nearly one-dimensional.

Static solutions do not depend on time and furthermore we are ultimately interested in background scalar fields which have non-trivial dependence on a single extra dimension. Thus we seek solutions to a set of coupled field equations which depend only on one spatial dimension, call it z and denote the associated derivative by prime. The numerical relaxation procedure outlined in Section A.2 will be used exclusively for finding these solutions.

Arbitrary initial conditions to a field equation will generally lead to a temporal evolution. Static solutions are those which remain constant over time. The perturbative stability of a static solution can be determined by investigating the temporal evolution of initial conditions which differ slightly from the static solution. If the field equations show the time dependent solution oscillating about, or returning to the static solution, then we can be assured of stability. The field equation for such a perturbation comes from the substitution

$$\phi \to [P(z) + p(t,z)] + \mathrm{i}\,[Q(z) + q(t,z)]\,, \tag{8}$$

where we have used a cartesian decomposition[7] for a complex scalar field ϕ. The perturbations p and q are much smaller than the static solutions P and Q and we work only to first order in calculations involving this decomposition.

The field equations we will be working with are all similar to the Klein-Gordon equation in that the second derivative is taken with respect to all dimensions and is linear. The fields all depend on the z spatial dimension and the perturbations also depend on time. In general, after making the substitution (8) we get pairs of equations for the real and imaginary perturbations

$$\begin{aligned}\left(\partial_z^2 - F_1(z)\right) p - G_1(z) q &= \partial_t^2 p,\\ \left(\partial_z^2 - F_2(z)\right) q - G_2(z) p &= \partial_t^2 q,\end{aligned}$$

where F_i and G_i are known functions of the static solutions P and Q which change only with z. In order to simplify things, we consider decoupled perturbations where only one of the fields is perturbed at anyone time. Thus the G_i can be discarded and we have equations for p and q which can be turned into eigenfunction problems. To do so, in a similar way to [15], we look for normal

[7] We use cartesian instead of polar complex decomposition to eliminate singularities at $r = 0$ which complicate the numerical calculations.

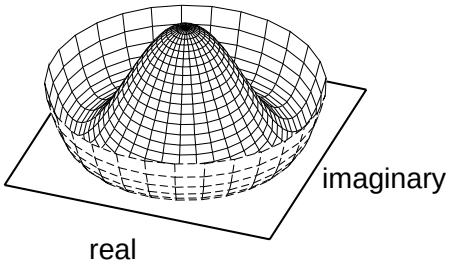

Figure 5: The mexican hat potential – a quartic potential for a complex valued scalar field with a continuously connected ring of minima.

modes of the form

$$p(t, z) = p(z)\mathrm{e}^{\mathrm{i}\omega t}, \tag{9}$$

where ω is the eigenvalue corresponding to the eigenfunction $p(z)$. Making this substitution for p yields

$$\left(-\tfrac{\mathrm{d}^2}{\mathrm{d}z^2} + F_1(z)\right) p = \omega^2 p.$$

A similar equation holds for the imaginary component. In general, this equation must be solved numerically and we use the eigensystem technique described in Section A.1 for this. If $\omega^2 \geq 0$ then ω is real and the perturbation will oscillate, meaning the static solution is stable. Alternatively, if ω is imaginary, the perturbations blow up and the static solution is unstable.

4 Scalar field with a quartic potential

To begin with we analyse the stability of a single complex valued scalar field in a quartic potential. A complex field is the next step up from the real scalar field studied in Section 2 and while the potential has a very similar mathematical form

$$V(\phi) = \lambda(\phi^*\phi - v^2)^2, \tag{10}$$

it is topologically different, as shown in Figure 5. Whereas a real quartic has two disconnected minima, the complex version has a continuously connected ring of minima at $\phi = v$. This difference leads to an unstable domain wall solution, as we shall now show.

Beginning from the Lagrangian as before, we make a complex generalisation of (3)

$$\mathcal{L} = (\partial^\mu\phi)^*\, \partial_\mu\phi - V(\phi),$$

where V is the mexican hat potential (10). Varying the action associated with this Lagrangian and making it stationary, yields the equation of motion for ϕ

$$\partial^\mu\partial_\mu\phi = -\frac{\partial V}{\partial\phi^*}. \tag{11}$$

To find the static solutions we assume dependence only on z and make the cartesian decomposition $\phi = P + \mathrm{i}Q$. This leads to two equivalent equations for the real and imaginary parts. For finite energy solutions we must have

the potential minimised as z tends to infinity and so we choose the convenient boundary conditions $P \to \pm v$ and $Q \to 0$. This leads to $Q = 0$ everywhere and an equation for the static real part

$$P'' = 2\lambda P(P^2 - v^2),$$

which is equivalent to the real case, the solution given by (5).

4.1 Stability analysis

Following the procedure outlined in Section 3 we make small time dependent perturbations, p and q, on the known static solutions. Looking for normal modes, we obtain the eigenvalue equations for decoupled perturbations

$$\left(-\tfrac{\mathrm{d}^2}{\mathrm{d}z^2} + 2\lambda(3P^2 - v^2)\right) p = \omega_p^2 p,$$
$$\left(-\tfrac{\mathrm{d}^2}{\mathrm{d}z^2} + 2\lambda(P^2 - v^2)\right) q = \omega_q^2 q.$$

For this simple case, we are able to find analytic solutions for both the eigenvalues and eigenfunctions[8]. The eigenvalues for the real and imaginary perturbation are

$$\omega_p^2 = 0,\ 3\lambda v^2 \text{ and } 4\lambda v^2,$$
$$\omega_q^2 = -\lambda v^2 \text{ and } 0.$$

The largest eigenvalue in each set corresponds to an unbound state. The associated eigenfunctions are

$$p_{(\omega^2=0)} = \sqrt{3/32}\left(1 - \tanh^2(\sqrt{\lambda}\, vz)\right),$$
$$p_{(\omega^2=3\lambda v^2)} = \sqrt{3/16}\frac{\tanh(\sqrt{\lambda}\, vz)}{\cosh(\sqrt{\lambda}\, vz)},$$
$$q_{(\omega^2=-\lambda v^2)} = \sqrt{1/16}\frac{1}{\cosh(\sqrt{\lambda}\, vz)},$$

with the coefficients just a normalisation. For the unbound states we get the following differential equations

$$\left(-\tfrac{\mathrm{d}^2}{\mathrm{d}z^2} + 6\lambda v^2(\tanh^2(\sqrt{\lambda}\, vz) - 1)\right) p_{(\omega^2=4\lambda v^2)} = 0,$$
$$\left(-\tfrac{\mathrm{d}^2}{\mathrm{d}z^2} + 2\lambda v^2(\tanh^2(\sqrt{\lambda}\, vz) - 1)\right) q_{(\omega^2=0)} = 0,$$

which have the solutions[9]

$$p_{(\omega^2=4v^2)} = 2 - \frac{3}{\cosh^2(\sqrt{\lambda}\, vz)},$$
$$q_{(\omega^2=0)} = \tanh(\sqrt{\lambda}\, vz).$$

[8] We achieved this by first solving numerically and then guessing a fit to the data, which verifies our computational method, at least in this case.

[9] These may or may not be unique solutions.

We analyse the stability of the static domain wall by looking at the sign of the eigenvalues. Both the real and imaginary perturbations have a zero mode with $\omega^2 = 0$. This corresponds to the physical property of translation invariance of the equations. If the domain wall is given some initial "kick" then it will propagate through space but will retain its shape. The other eigenvalues of p are all positive and so the real component of the kink is stable. This is not so for the imaginary part since there is a negative eigenvalue $\omega^2 = -v^2\lambda$; any perturbation that has a component in the imaginary direction will cause the entire kink to collapse. We conclude that the domain wall created by the mexican hat potential is *unstable*.

4.2 Time evolution

To obtain a qualitative feel of the instability of our domain wall, we go back to (11) and solve the field equations with t and z dependence. With the decomposition $\phi = r_1(t,z) + \mathrm{i}\, r_2(t,z)$ we get two equivalent equations

$$\left(\tfrac{\partial^2}{\partial z^2} - \tfrac{\partial^2}{\partial t^2}\right) r_i = 2\lambda r_i \left(r_1^2 + r_2^2 - v^2\right).$$

By employing the techniques described in Appendix A.3, we are able to numerically time integrate these equations and watch the kink decay after a small perturbation. Figure 6 shows a time sequence of the numerical solutions. The initial condition is that of a real valued static kink interpolating from $-v$ to v. A small perturbation is applied to the imaginary part which begins as all zero, but eventually grows to v while the real part decays. As the eigenvalue analysis established, this kink is unstable and we see this verified in the temporal solutions.

As a further aid to visualisation, we plot the kink on a graph of the mexican hat potential, see Figure 7. The two end points in the valley depict the kink asymptoting to $\pm v$. It is immediately obvious as to the nature of the instability – the ring of minima is a much more energetically favourable place for the solution to lie. The initial energy from the static solution is now in the form of momentum and as time evolves, the solution continues to oscillate in the valley. Due to the dynamics of this situation, the kink will not form again at the top of the potential hill and so the perturbation has destroyed the domain wall.

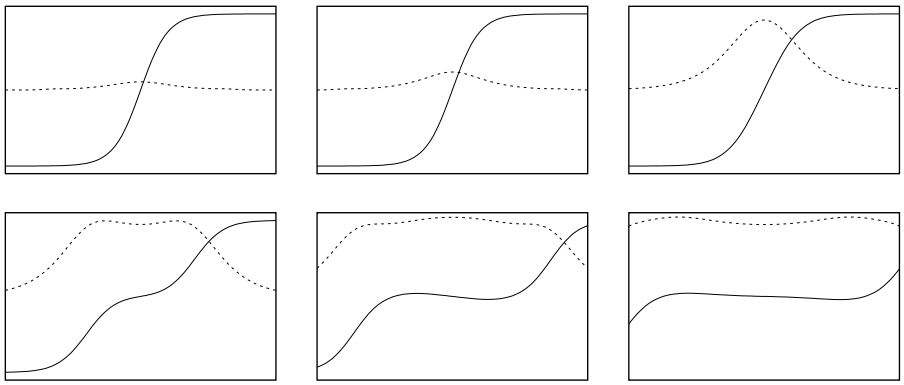

Figure 6: A time sequence (read left to right, top to bottom) of a small perturbation applied to the static domain wall with the mexican hat potential. The solid line is the real part, the dashed line is the imaginary part; the initial condition is an all real kink. The perturbation is applied to the imaginary component and since the static solution is *unstable* the real part becomes all positive and the domain wall decays.

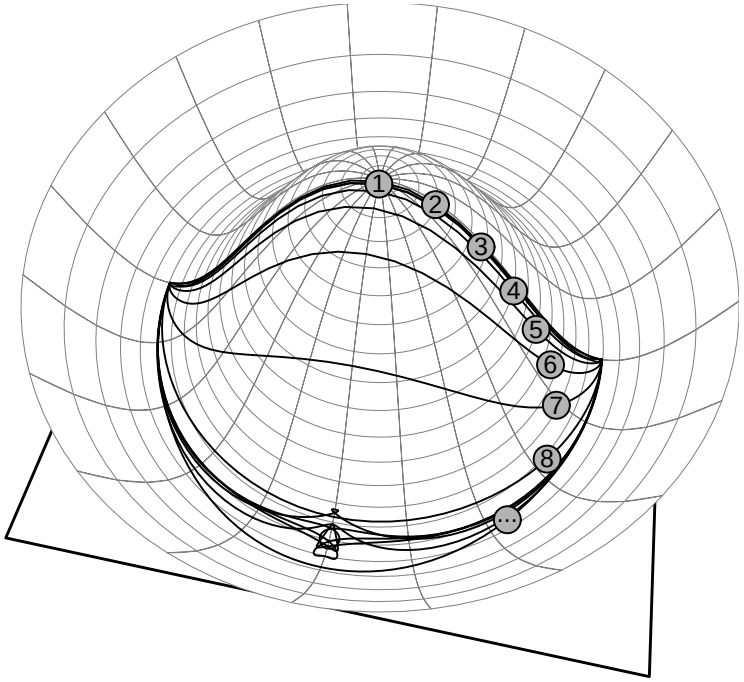

Figure 7: A 3D visualisation of Figure 6. The domain wall static solution is stretched over the mexican hat potential and shows clearly why the kink is unstable. As time evolves, the solution oscillates indefinitely in the valley and does not form back into a domain wall. The numbers label the time sequence and the base plane represents the real and imaginary components of ϕ.

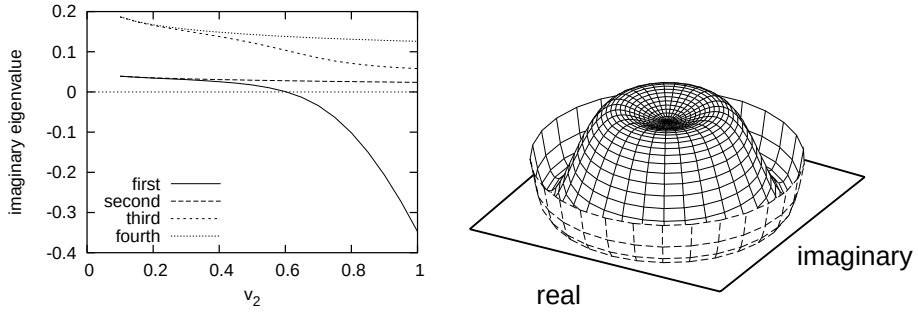

Figure 8: On the left are the first four eigenvalues of the imaginary perturbation for a sextic potential, plotted against the parameter v_2. We have $\lambda = v_1 = 1$. For the region $v_2 \gtrsim 0.6$ the first eigenvalue is negative and so the domain wall is unstable. The potential in this situation is shown on the right. When the dip in the centre is deep enough, the domain wall is perturbatively stable.

5 Scalar field with a sextic potential

In this section we briefly discuss the behaviour of a potential which allows a perturbatively stable domain wall for a certain parameter range. Such a potential is the sextic

$$V(\phi) = \lambda(\phi^*\phi - v_1^2)^2(\phi^*\phi + v_2^2),$$

where v_1 and v_2 can be tuned to give stable or unstable static solutions. As before, we find the static solutions by cartesian decomposition and take the imaginary part to be zero. The equation for the real part is

$$P'' = 2\lambda P(P^2 - v_1^2)(P^2 + v_2^2) + \lambda P(P^2 - v_1^2)^2, \tag{12}$$

and the decoupled perturbation equations are

$$\begin{aligned} \left(-\tfrac{\mathrm{d}^2}{\mathrm{d}z^2} + 4\lambda P(3P^2 - 2v_1^2 + v_2^2) + 2\lambda(P^2 - v_1^2)(2P^2 - v_1^2 + v_2^2)\right) p &= \omega^2 p, \\ \left(-\tfrac{\mathrm{d}^2}{\mathrm{d}z^2} + 2\lambda(P^2 - v_1^2)(2P^2 - v_1^2 + v_2^2)\right) q &= \omega^2 q. \end{aligned} \tag{13}$$

For this case we are not able to find an analytic form of the static solution or analytic eigenvalues and eigenfunctions. We must instead compute the real static component P by using the relaxation method on (12) and then use the resulting numerical approximation in (13).

All of the eigenvalues for the real perturbation are found to be positive, so do not contribute to any instability. The eigenvalues for the imaginary perturbation are show on the left in Figure 8; they are plotted against the parameter v_2. The smallest eigenvalue is just slightly positive for $v_2 \lesssim 0.6$ and so the domain wall is perturbatively stable in this case. When v_2 is large enough, the dip in the sextic potential, see the right of Figure 8, is not deep enough to prevent the kink from finding the ring of minima and the static domain wall solution is unstable.

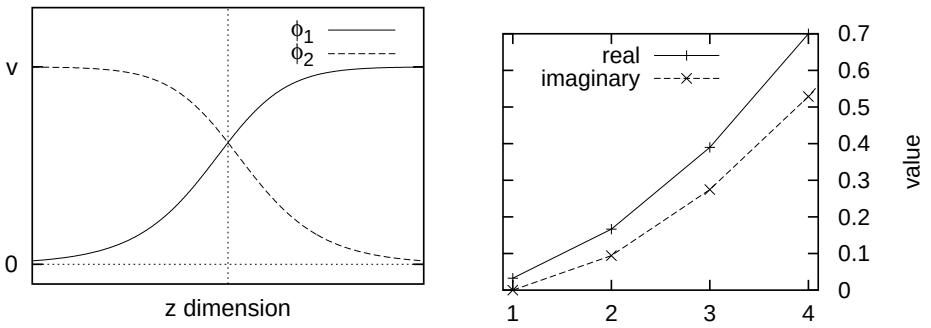

Figure 9: On the left are the static solutions for the two scalar field "clash of symmetries" scenario. On the right are the eigenvalues for perturbations of this domain wall. There are no negative eigenvalues so the wall is stable.

6 Two scalar fields – clash of symmetries

In the Rozowsky et al. model there are two complex scalar fields, ϕ_1 and ϕ_2. The motivation for this comes from the "clash of symmetries" idea (see [16]) where a Lagrangian with multiple scalar fields is endowed with a discrete symmetry whereby it remains invariant under a permutation of the scalars. A large continuous global vacuum symmetry is then broken down into smaller, equivalent, but differently embedded subgroups. Each scalar field then interpolates between these different smaller vacua such that the discrete permutation symmetry is preserved.

Before we study the stability of the full Rozowsky et al. model, we look at it with gauge fields absent. The Lagrangian, which has a $\phi_1 \leftrightarrow \phi_2$ interchange symmetry, is

$$\mathcal{L} = (\partial^\mu \phi_1)^* \, \partial_\mu \phi_1 + (\partial^\mu \phi_2)^* \, \partial_\mu \phi_2 - V(\phi_1, \phi_2). \tag{14}$$

There are restrictions on the potential for it to remain invariant under the discrete $\mathbb{Z}_2$ transformation of the scalar fields. A quartic potential with this symmetry property that is used in the full gauge field model is

$$V(\phi_1, \phi_2) = \lambda_1(\phi_1^*\phi_1 + \phi_2^*\phi_2 - v^2)^2 + \lambda_2 \phi_1^*\phi_1\phi_2^*\phi_2, \tag{15}$$

where λ_1, λ_2 and v are positive parameters. The equations of motion are

$$\partial^\mu \partial_\mu \phi_a = -\frac{\partial V}{\partial \phi_a^*},$$

where $a = 1, 2$ is the field index. The boundary conditions must again minimise the potential and also be compatible with the "clash of symmetries" $\mathbb{Z}_2$ discrete symmetry. To achieve this we look for solutions with $\phi_1^*\phi_1$ interpolating between 0 and v^2 and $\phi_2^*\phi_2$ between v^2 and 0. The solutions, shown on the left in Figure 9, are two symmetric domain walls meeting – they clash at the origin.

We perform perturbative stability analysis as in the previous sections and obtain the first 4 eigenvalues for the real and imaginary components, shown on the right in Figure 9. Note that the eigenvalues are the same for both fields, as they respect a $\mathbb{Z}_2$ symmetry. Since all eigenvalues are positive, the

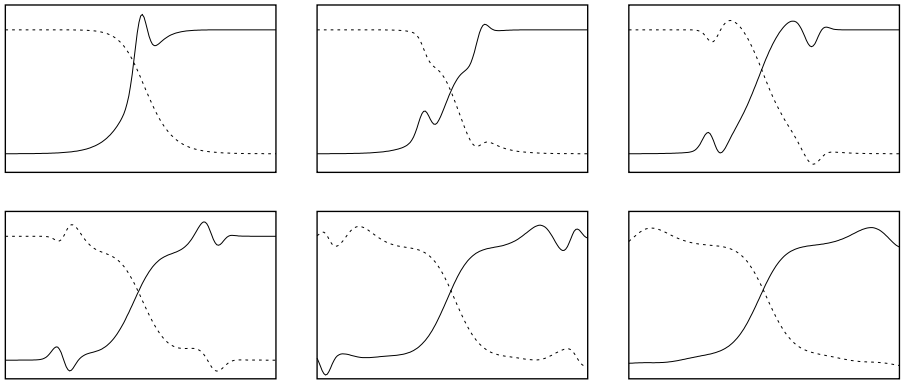

Figure 10: A time sequence of a perturbation of the domain wall created by the clash of two complex valued scalar fields in a quartic potential. In contrast to Figure 6 where there was only a single scalar field, this domain wall solution is stable. The perturbation evolves like a wave on a string and heads off to infinity, leaving the two scalar fields to return to their original form.

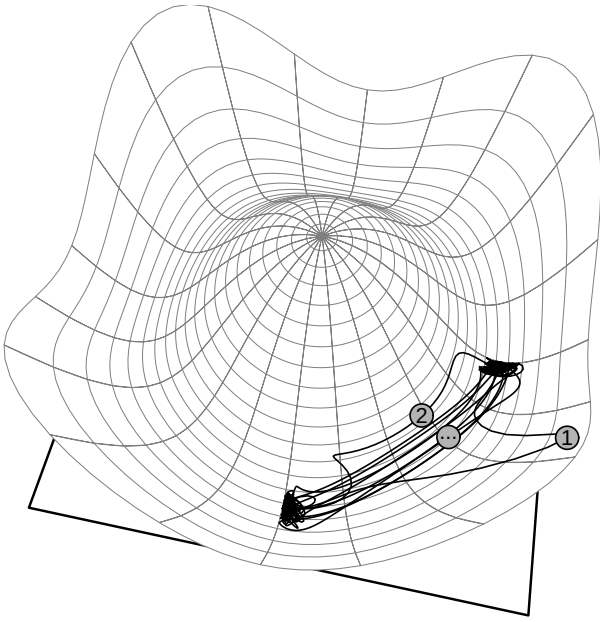

Figure 11: This alternative visualisation of Figure 10 shows that the domain wall is stable because it is lying in a potential valley. The perturbation kicks one of the scalar fields up the side of this valley and it proceeds to oscillate with a decreasing amplitude, eventually returning to its orginial form. The numbers label the time sequence and the base plane represents the $|\phi_1|$ and $|\phi_2|$ axis.

domain wall is stable and this is verified again by the temporal evolution of the solutions, shown in Figures 10 and 11. The visualisation of the domain wall in the potential shows that the static solution lies in a valley and so is already in the most energetically favourable configuration.

7 Two scalar fields with two gauge fields

Now we move on to the full $U(1) \otimes U(1)$ model proposed by Rozowsky et al. As a direct extension of the simple clash of symmetries model given by (14), the Lagrangian is obtained by adding $\mathbb{Z}_2$ symmetry preserving Abelian gauge fields, coupled to the scalar fields. This yields

$$\mathcal{L} = (\mathcal{D}^\mu \phi_1)^* \mathcal{D}_\mu \phi_1 + (\mathcal{D}^\mu \phi_2)^* \mathcal{D}_\mu \phi_2 - \tfrac{1}{4} \mathcal{F}_1^{\mu\nu} \mathcal{F}_{1\mu\nu} - \tfrac{1}{4} \mathcal{F}_2^{\mu\nu} \mathcal{F}_{2\mu\nu} - V(\phi_1, \phi_2), \quad (16)$$

where the potential is quartic, as defined by (15). The two Abelian gauge fields $\mathcal{A}_1^\mu$ and $\mathcal{A}_2^\mu$ are introduced in the usual way by the antisymmetric tensor

$$\mathcal{F}_a^{\mu\nu} = \partial^\mu \mathcal{A}_a^\nu - \partial^\nu \mathcal{A}_a^\mu.$$

The covariant derivative is

$$\mathcal{D}^\mu = \partial^\mu - \mathrm{i} Q_1 \mathcal{A}_1^\mu - \mathrm{i} Q_2 \mathcal{A}_2^\mu,$$

where Q_a is the charge operator associated with the scalar field ϕ_a. Keeping the discrete symmetry, the $U(1) \otimes U(1)$ charges of the scalar fields are $\phi_1 \sim (e, \tilde{e})$ and $\phi_2 \sim (\tilde{e}, e)$, with e and $\tilde{e}$ constants. We note that in the Rozowsky et al. model, $\tilde{e} = 0$. The covariant derivative applied to each scalar field is then

$$\begin{aligned} \mathcal{D}^\mu \phi_1 &= \partial^\mu \phi_1 - \mathrm{i} e \mathcal{A}_1^\mu \phi_1 - \mathrm{i} \tilde{e} \mathcal{A}_2^\mu \phi_1, \\ \mathcal{D}^\mu \phi_2 &= \partial^\mu \phi_2 - \mathrm{i} \tilde{e} \mathcal{A}_1^\mu \phi_2 - \mathrm{i} e \mathcal{A}_2^\mu \phi_2. \end{aligned}$$

Applying the Euler-Lagrange equation (1) to the scalar and gauge fields, gives the ten equations of motion

$$\begin{aligned} \mathcal{D}^\mu \mathcal{D}_\mu \phi_a &= -2\lambda_1 \phi_a (\phi_a^* \phi_a + \phi_b^* \phi_b - v^2) - \lambda_2 \phi_a \phi_b^* \phi_b, \\ \partial_\nu \mathcal{F}_a^{\nu\mu} &= 2 \operatorname{Im} \left(e \phi_a^* \mathcal{D}^\mu \phi_a + \tilde{e} \phi_b^* \mathcal{D}^\mu \phi_b \right), \end{aligned} \quad (17)$$

where $a = 1$ and $b = 2$, or $a = 2$ and $b = 1$. As in the previous sections we look for solutions that depend only on z. Unlike the previous sections, we initially perform a polar decomposition of the complex fields, $\phi_a = R_a \mathrm{e}^{\mathrm{i}\theta_a}$ which greatly simplifies the static solutions. Since we are working with gauge fields, we have the freedom to choose two gauges, one for each $\mathcal{A}_a^\mu$, and the Lorentz gauge turns out to be the most suitable choice, $\partial_\mu \mathcal{A}_a^\mu = 0$. Under these conditions, the field equations of motion (17) reduce to

$$\begin{aligned} R_a'' &= -R_a \left((e\mathcal{A}_a^t + \tilde{e}\mathcal{A}_b^t)^2 - (e\mathcal{A}_a^x + \tilde{e}\mathcal{A}_b^x)^2 - (e\mathcal{A}_a^y + \tilde{e}\mathcal{A}_b^y)^2 \right) \\ &\quad + 2\lambda_1 R_a (R_a^2 + R_b^2 - v^2) + \lambda_2 R_a R_b^2, \\ \mathcal{A}_a^{(t,x,y)\prime\prime} &= 2eR_a^2 (e\mathcal{A}_a^{(t,x,y)} + \tilde{e}\mathcal{A}_b^{(t,x,y)}) + 2\tilde{e}R_b^2 (e\mathcal{A}_b^{(t,x,y)} + \tilde{e}\mathcal{A}_a^{(t,x,y)}), \\ \theta_a' &= -(e\mathcal{A}_a^z + \tilde{e}\mathcal{A}_b^z). \end{aligned} \quad (18)$$

We now see why a polar decomposition was helpful; in the Lorentz gauge the $\mathcal{A}_a^z$ are constant and so the phase of each scalar field is linear in z. Thus the two amplitudes R_a decouple nicely from their respective θ_a and we only need to solve the first two equations in (18). A further simplification is to note that the equations for the $\mathcal{A}_a^\rho$, where $\rho = t, x, y$, are all equivalent and the linear

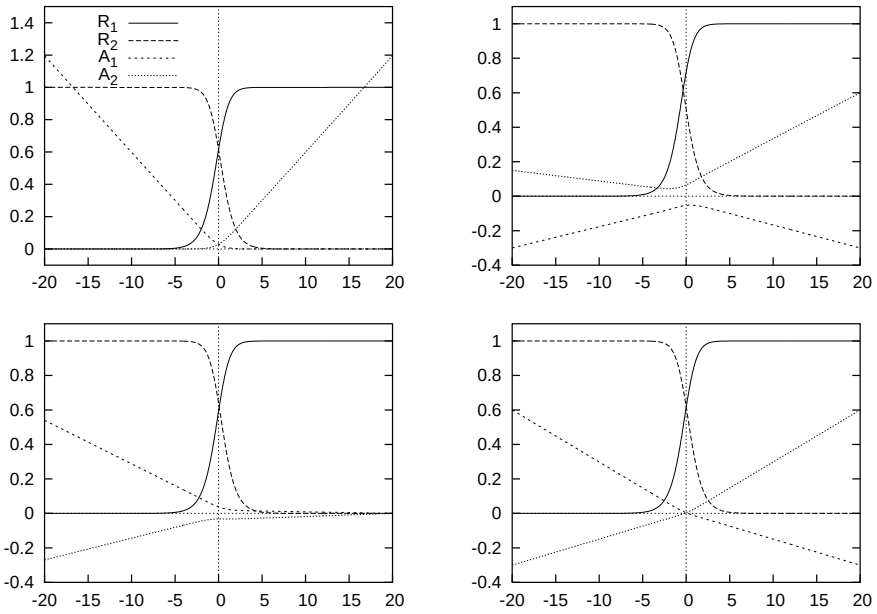

Figure 12: Static solutions to the two scalar and two gauge fields in the $U(1) \otimes U(1)$ model. In all cases $\lambda_1 = \lambda_2 = v = e = 1$. In the top left plot, $\tilde{e} = 0$ as in the Rozowsky et al. model and the gauge fields show Meisner-like suppression under their respective scalar field. In the other three plots, $\tilde{e} = \frac{1}{2}$ and we show cases with various values for the free gauge field boundary conditions.

combination $(e\mathcal{A}^{\rho}_{a} + \tilde{e}\mathcal{A}^{\rho}_{b})$ is present in the equations for the R_a in a pseudo-Euclidean distance form. By choosing to only measure this distance, denoted by A_a, the equations become

$$R_a'' = R_a(eA_a + \tilde{e}A_b)^2 + 2\lambda_1 R_a(R_a^2 + R_b^2 - v^2) + \lambda_2 R_a R_b^2, \tag{19a}$$

$$A_a'' = 2eR_a^2(eA_a + \tilde{e}A_b) + 2\tilde{e}R_b^2(eA_b + \tilde{e}A_a). \tag{19b}$$

Remembering that a and b can alternate between 1 and 2, we have four degrees of freedom to solve for; the two scalar field magnitudes R_1 and R_2 and the two gauge fields A_1 and A_2. The boundary conditions for the R_a are the same as those given in Section 6; $R_1 \to 0$ and $R_2 \to v$ as $z \to -\infty$ and $R_1 \to v$ and $R_2 \to 0$ as $z \to \infty$. With these conditions, equation (19a) forces $(eA_2 + \tilde{e}A_1) \to 0$ as $z \to -\infty$ and $(eA_1 + \tilde{e}A_2) \to 0$ as $z \to \infty$. These linear combinations leave two degrees of freedom for our boundary conditions. Subsequently, these conditions combined with equation (19b) forces $A_a'' \to 0$ as $z \to \pm\infty$, so the gauge fields are asymptotically linear.

We use the relaxation procedure outlined in Appendix A.2 to solve the set of four coupled differential equations given by (19) subject to the aforementioned boundary conditions. Results are shown in Figure 12 with $\lambda_1 = \lambda_2 = v = 1$. The top left plot has $e = 1$ and $\tilde{e} = 0$ and shows equivalent results to those obtained in [1]. The other three plots have $e = 1$ and $\tilde{e} = \frac{1}{2}$ and show results for various values of the two free boundary conditions for the A_a. In all cases the scalar fields clash and form a domain wall between the two vacua. The form of

the gauge fields is reminiscent of the Meisner effect; for the $\tilde{e} = 0$ case they are suppressed on the side which has their corresponding scalar field asymptoting to v. This can also be viewed as semi-localisation of the gauge fields to the brane, a mechanism that may lead to full gauge field localisation in a more sophisticated model.

7.1 Stability analysis

Similar to previous sections, we perform stability analysis of the static solutions described by (19). Polar decomposition of the complex fields does not lend itself to clean numerical work due to singularities in the magnitude. We thus begin from (17) and derive equations for a cartesian decomposition $\phi_a = P_a + \mathrm{i}Q_a$. For simplicity we set $\tilde{e} = 0$ and by the same argument as before, only consider the combination of $\mathcal{A}_a^{(t,x,y)}$ denoted A_a. Since we are working with the real and imaginary components of the scalar fields, we will have terms involving $\mathcal{A}_a^z$ which we have shown previously to be constant in the Lorentz gauge; we denote this constant $\mathcal{A}_a^z$ by Z_a. The equations for the static solutions are then

$$\begin{aligned} P_a'' &= 2eZ_aQ_a' + e^2P_a(A_a^2 + Z_a^2) \\ &\quad + 2\lambda_1 P_a(P_a^2 + Q_a^2 + P_b^2 + Q_b^2 - v^2) + \lambda_2 P_a(P_b^2 + Q_b^2), \\ Q_a'' &= -2eZ_aP_a' + e^2Q_a(A_a^2 + Z_a^2) \\ &\quad + 2\lambda_1 Q_a(P_a^2 + Q_a^2 + P_b^2 + Q_b^2 - v^2) + \lambda_2 Q_a(P_b^2 + Q_b^2), \\ A_a'' &= 2e^2(P_a^2 + Q_a^2)A_a. \end{aligned} \tag{20}$$

We add to the static fields P_a, Q_a and A_a a small time dependent perturbation p_a, q_a and a_a respectively. Substituting this decomposition into the original field equations (17) and using the equations for the static fields (20), we arrive at the eigenvalue equations

$$\begin{aligned} \Big(-\tfrac{\mathrm{d}^2}{\mathrm{d}z^2} + e^2(A_a^2 + Z_a^2) \\ +2\lambda_1(3P_a^2 + Q_a^2 + P_b^2 + Q_b^2 - v^2) + \lambda_2(P_b^2 + Q_b^2)\Big)p_a &= \omega^2 p_a, \\ \Big(-\tfrac{\mathrm{d}^2}{\mathrm{d}z^2} + e^2(A_a^2 + Z_a^2) \\ +2\lambda_1(P_a^2 + 3Q_a^2 + P_b^2 + Q_b^2 - v^2) + \lambda_2(P_b^2 + Q_b^2)\Big)q_a &= \omega^2 q_a, \\ \Big(-\tfrac{\mathrm{d}^2}{\mathrm{d}z^2} + 2e^2(P_a^2 + Q_a^2)\Big)\, a_a &= \omega^2 a_a. \end{aligned}$$

A solution to the static equations with cartesian decomposition is shown in Figure 13 and since $Z_a \neq 0$ for this case, the phase of the scalar field increases linearly and the real and imaginary parts oscillate. Only one set of the fields are shown in the figure, the other three are just a reflection about $z = 0$. The eigenvalues for the perturbations are plotted in Figure 14 for $3 \times 4 \times 4$ different combinations of v, λ_1 and λ_2 respectively. For all cases the eigenvalues corresponding to p_a and q_a are positive and those for a_a are zero. We have thus shown that the scalar and gauge fields in the Rozowsky et al. $U(1) \otimes U(1)$ model are stable.

In addition to the eigenvalue analysis, we also perform a full time evolution of the scalar and gauge fields. We go back to the original equations of motion (17),

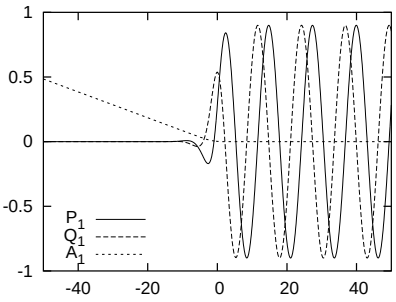

Figure 13: Solutions to the static $U(1)\otimes U(1)$ equations with cartesian decomposition. The parameters are $e = 1$, $\tilde{e} = 0$, $v = 0.9$, $\lambda_1 = 1.1$, $\lambda_2 = 0.3$, $A'_a \to 0.01$ and $Z_a = 0.5$. Since $Z_a \neq 0$ the real and imaginary parts oscillate. The other three fields are just reflected about $z = 0$.

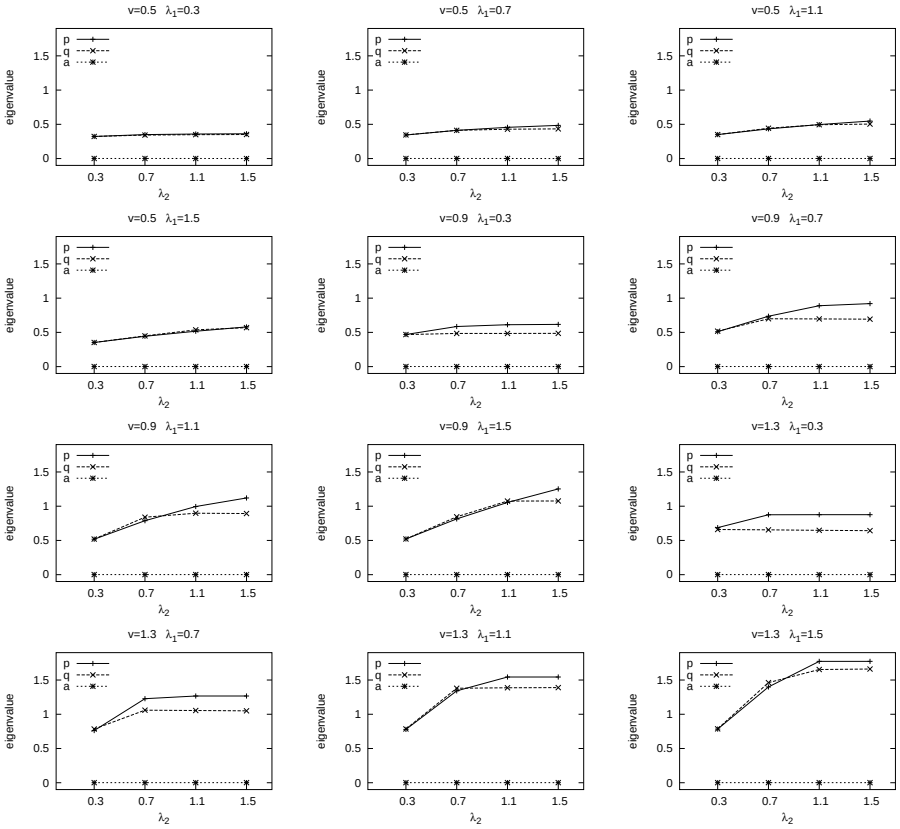

Figure 14: The eigenvalues for the real, p, and imaginary, q, parts of a perturbation of the scalar fields and that for the gauge fields, a. All eigenvalues are non-negative and so all fields are independently stable. The common parameters are $e = 1$, $\tilde{e} = 0$, $A'_a \to 0.01$ and $Z_a = 0.5$. The other three parameters, λ_1, λ_2 and v take values as labelled in the plots.

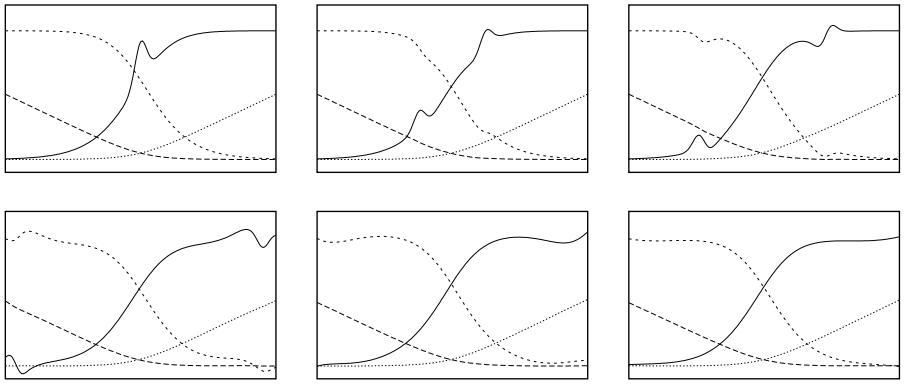

Figure 15: Time sequence of a perturbation of the scalar field in the $U(1) \otimes U(1)$ model. The perturbation heads off to infinity, leaving the fields to return to their stable configuration.

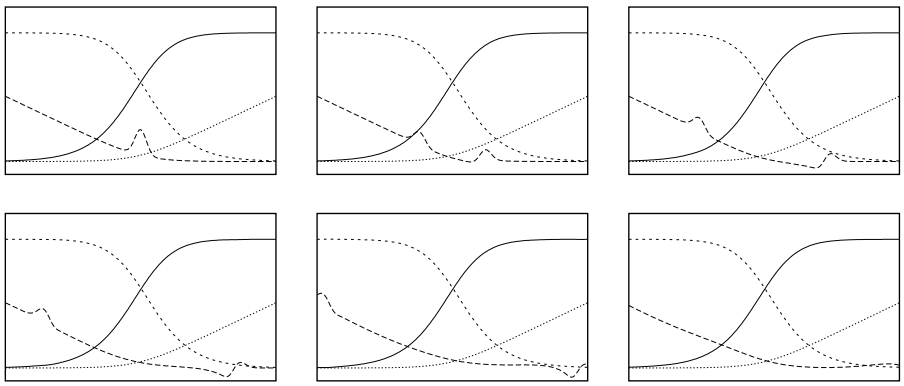

Figure 16: Time sequence of a perturbation of the gauge field in the $U(1) \otimes U(1)$ model. Again, the fields are all stable.

allow the fields to vary in the t and z dimensions and solve the resulting partial differential equations with the technique outlined in Appendix A.3. We choose the parameters $\lambda_1 = \lambda_2 = v = e = 1$ and $\tilde{e} = 0$; the initial conditions are similar to those in the top left plot in Figure 12. We apply a small perturbation to one of the scalar fields and as Figure 15 shows, all fields return to their original form – they are stable. Figure 16 tells a similar story for a perturbation of one of the gauge fields; the configuration is stable and returns to the static solution. The energy required for a perturbation travels off in both directions to infinity as a disturbance in the fields, leaving the domain wall intact.

With knowledge that the $U(1) \otimes U(1)$ model can describe a stable domain wall, it is possible to proceed to a more sophisticated set of fields and associated interactions. Interesting extensions would include full localisation of the gauge fields to the domain wall; non-Abelian gauge fields; a larger vacuum symmetry with more scalar fields; fermionic fields, their interactions and confinement; and as we discuss in the next section, gravity.

8 Gauge fields with gravity

One very important extension to the $U(1) \otimes U(1)$ model, in line with the work of Randall and Sundrum and other related studies, is the inclusion of gravity. By combining the simple warped metric action given by (7) and the $U(1) \otimes U(1)$ Lagrangian (16), we obtain the five dimensional action for our theory

$$S = \int \left(\kappa R + g^{AB} t_{AB} + \tfrac{1}{4} g^{AC} g^{BD} f_{ABCD} + V\right) \sqrt{-g}\, d^5x,$$

where we are now using the metric signature $(-,+,+,+,+)$, hence the difference in signs. The scalar and gauge kinetic terms are

$$\begin{aligned} t_{AB} &= (\mathcal{D}_A \phi_1)^* \mathcal{D}_B \phi_1 + (\mathcal{D}_A \phi_2)^* \mathcal{D}_B \phi_2, \\ f_{ABCD} &= \mathcal{F}_{1,AB} \mathcal{F}_{1,CD} + \mathcal{F}_{2,AB} \mathcal{F}_{2,CD}, \end{aligned}$$

with the usual covariant derivative and antisymmetric gauge tensor defined as

$$\begin{aligned} \mathcal{D}_A &= \partial_A - \mathrm{i} Q_1 \mathcal{A}_{1,A} - \mathrm{i} Q_2 \mathcal{A}_{2,A}, \\ \mathcal{F}_{a,AB} &= \partial_A \mathcal{A}_{a,B} - \partial_B \mathcal{A}_{a,A}. \end{aligned}$$

With the charge operator Q_a acting as in the $U(1) \otimes U(1)$ model. The potential is taken from [17] where the aim was to engineer V for two scalar fields, which lent itself to an analytic solution for the warped metric without a cuspy $-|w|$ term. As a consequence, V takes the rather unwieldy form

$$\begin{aligned} V = {} & \tfrac{-\beta^2 v^4}{12\kappa} + \tfrac{\beta^2}{v^2}\left(1 + \tfrac{u^2}{3\kappa}\right)\phi_1^2\phi_2^2 - \tfrac{2\beta^2}{v^4}\left(\tfrac{3}{2} + \tfrac{v^2}{3\kappa}\right)\phi_1^2\phi_2^2\left(\phi_1^2 + \phi_2^2 - v^2\right) \\ & + \zeta \tfrac{\beta^2}{2v^2}\left(\tfrac{3}{2} + \tfrac{v^2}{3\kappa}\right)\left(\phi_1^2 + \phi_2^2 - v^2\right)^2 \left(\eta + \tfrac{1}{v^2}\left(\phi_1^2 + \phi_2^2 - v^2\right)\right), \end{aligned}$$

where $\phi_a^2 = \phi_a^* \phi_a$ and β, ζ, η, v are constants. The equations of motion are given by the five dimensional Einstein equation (6) with the stress energy tensor

$$T_{AB} = 2t_{AB} + g^{CD} f_{ACBD} - g_{AB}\left(g^{CD} t_{CD} + \tfrac{1}{4} g^{CE} g^{DF} f_{CDEF} + V\right).$$

For the scalar and gauge fields we have

$$\begin{aligned} \mathcal{D}_A\left(\sqrt{-g}\, g^{AB} \mathcal{D}_B \phi_a\right) &= \sqrt{-g} \frac{\partial V}{\partial \phi_a^*}, \\ \partial_C\left(\sqrt{-g}\, g^{AB} g^{CD} \mathcal{F}_{a,BD}\right) &= \sqrt{-g}\, g^{AB} 2 \operatorname{Im}\left(e \phi_a^* \mathcal{D}_B \phi_a + \tilde{e} \phi_b^* \mathcal{D}_B \phi_b\right). \end{aligned}$$

For the static case, we again look for solutions that depend only on the extra dimension w. We must also choose a form for the metric in order to simplify the number of equations to solve, because at present there are $15 + 4 + 10$ unknown real fields for g_{AB}, ϕ_a and $\mathcal{A}_{a,A}$ respectively. As a generalisation of the RS model, we make the metric ansatz

$$\mathrm{d}s^2 = -e^{f(w)} dt^2 + e^{h(w)}(dx^2 + dy^2 + dz^2) + dw^2,$$

which allows the time and space dimensions to behave differently in the bulk. We use a polar decomposition for the scalar fields, $\phi_a = R_a \mathrm{e}^{\mathrm{i}\theta_a}$ and choose to only measure the t and w components of $\mathcal{A}_{a,A}$. As before, the Lorentz gauge leads to a static w gauge field component and the phase θ_a decouples from the

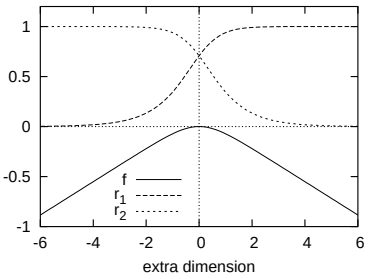

Figure 17: Analytic solutions to the $U(1) \otimes U(1)$ model with gravity. This is very similar to Figure 4 except we now have two scalar fields in a clash of symmetries. There are no gauge fields as the only static gauge field solution is the trivial one.

rest of the system. We are thus left with the six fields f, h, R_a and $\mathcal{A}_{a,t} = A_a$. We do not know the relative sizes of the gravity and matter fields because of the constant κ and so we must non-dimensionalise the equations. The metric functions are already dimensionless and the scalar and gauge fields have the same dimension; we use the length, L, and field, H, scales to define

$$y = \tfrac{w}{L}, \qquad r_a = \tfrac{R_a}{H}, \qquad a_a = \tfrac{A_a}{H}, \qquad \alpha = \tfrac{H^2}{\kappa},$$
$$\mu = \tfrac{u}{H}, \qquad \gamma = L\beta, \qquad \varepsilon = LHe, \qquad \tilde{\varepsilon} = LH\tilde{e}.$$

In terms of these dimensionless fields and parameters, the equations are

$$\begin{aligned}
r_a'' &= \tfrac{-1}{2}(f' + 3h')r_a' - \mathrm{e}^{-f}(\varepsilon a_a + \tilde{\varepsilon} a_b)^2 r_a - \tfrac{2\gamma^2}{\mu^4}(\tfrac{3}{2} + \tfrac{\alpha\mu^2}{3}) r_a r_b^2 (2r_a^2 + r_b^2 - \mu^2) \\
&\quad + \tfrac{\gamma^2}{\mu^2}(1 + \tfrac{\alpha\mu^2}{3}) r_a r_b^2 + \tfrac{\zeta\gamma^2}{2\mu^2}(\tfrac{3}{2} + \tfrac{\alpha\mu^2}{3}) r_a (r_a^2 + r_b^2 - \mu^2)(2\eta + \tfrac{3}{\mu^2}(r_a^2 + r_b^2 - \mu^2)), \\
a_a'' &= \tfrac{1}{2}(f' - 3h')a_a' + 2(\varepsilon^2 r_a^2 + \tilde{\varepsilon}^2 r_b^2) a_a + 2\varepsilon\tilde{\varepsilon}(r_a^2 + r_b^2) a_b, \\
h'' &= -h'^2 - \tfrac{1}{3}\Psi - \tfrac{1}{3}\Phi, \\
f'' &= -\tfrac{1}{2} f'^2 - h' f' + \tfrac{1}{2} h'^2 + \tfrac{5}{3}\Psi - \tfrac{1}{3}\Phi,
\end{aligned}$$

where prime denotes a derivative with respect to y and

$$\begin{aligned}
\Psi &= \alpha \mathrm{e}^{-f} \left(\tfrac{1}{2}(a_a'^2 + a_b'^2) + r_a^2(\varepsilon a_a + \tilde{\varepsilon} a_b)^2 + r_b^2(\varepsilon a_b + \tilde{\varepsilon} a_a)^2 \right), \\
\Phi &= \alpha(r_a'^2 + r_b'^2 - \tfrac{\alpha\gamma^2\mu^2}{12} + \tfrac{\gamma^2}{\mu^2}(1 + \tfrac{\alpha\mu^2}{3}) r_a^2 r_b^2 - \tfrac{2\gamma^2}{\mu^4}(\tfrac{3}{2} + \tfrac{\alpha\mu^2}{3}) r_a^2 r_b^2 (r_a^2 + r_b^2 - \mu^2) \\
&\quad + \tfrac{\zeta\gamma^2}{2\mu^2}(\tfrac{3}{2} + \tfrac{\alpha\mu^2}{3})(r_a^2 + r_b^2 - \mu^2)^2 (\eta + \tfrac{1}{\mu^2}(r_a^2 + r_b^2 - \mu^2))).
\end{aligned}$$

With $f = h$ and $a_a = 0$ there exists analytic solutions, shown in Figure 17, which take the form

$$f(y) = \tfrac{-\alpha\mu^2}{6} \log\left(\cosh(\gamma y)\right), \qquad r_{1,2}(y) = \tfrac{\mu}{\sqrt{2}} \sqrt{1 \pm \tanh(\gamma y)}.$$

We were able to obtain these solutions numerically and in fact these were the *only* solutions that arose in our numerical investigations; there were no non-trivial gauge solutions. We attempt to see this analytically by comparing the equation for a_a with and without gravity. Taking $\tilde{e} = 0$ for simplicity we have

$$a_a'' = \tfrac{1}{2}(f' - 3h')a_a' + 2\varepsilon^2 r_a^2 a_a, \tag{21}$$

where the first term on the right hand side is not present in the original $U(1) \otimes U(1)$ model. Without gravity, because $2\varepsilon^2 r_a^2 \geq 0$, the second derivative of a_a

must always have the same sign as a_a itself. Thus the function always turns away from the horizontal axis, resulting in all non-trivial solutions blowing up at infinity. We have the same conclusion when gravity is included, as any turning point of a_a, where $a'_a = 0$, must also turn away from the axis[10]. In the $U(1) \otimes U(1)$ model, a_a blew up linearly without any problems and we noted the similarity of this to the Meisner effect. By including gravity, the right hand side of equation (21) now tends to zero only if $(f' - 3h') \to 0$ or $a'_a \to 0$. The former case is inconsistent with asymptotic analysis of the equations for f and h, furthermore if $a'_a \nrightarrow 0$, Ψ blows up exponentially. We conclude that the only static solution for the gauge fields is the trivial one, $a_a = 0$.

9 Conclusion

In this thesis we began with a discussion of the historical development of the physics which led to the study of extra dimensions and showed that infinite extra dimensions are quite plausible. We then proceeded to give an overview of the more technical aspects of domain walls and demonstrated that a quartic scalar potential with distinct minima can support a kink solution. Einstein's theory in five dimensions was introduced in the context of a warped extra dimension. We gave an example of an action with gravity and a scalar field and presented a solution with approximate AdS_5 space in the bulk either side of a dynamically generated domain wall. Following this introductory material, we outlined the technique we developed to analyse the perturbative stability of static solutions; it was based on the signs of the eigenvalues of normal modes.

We applied our stability analysis technique to a quartic potential with a single complex valued field and showed that the domain wall was unstable. For this model we were able to find analytic eigenvalues and eigenfunctions, but in the other cases we relied on numerical methods. A scalar field with a sextic potential was shown to have a perturbatively stable domain wall solution for a certain range of a parameter in the potential. For the clash of symmetries model, we established the stability of the domain wall solution made of two scalar fields. Excluding the sextic potential, we also performed numerical time evolution of the field equations for each model, in order to gain a more intuitive understanding of their stability behaviour.

Our main results were establishing the stability of both the scalar and gauge fields of the Rozowsky et al. $U(1) \otimes U(1)$ model. We showed that the eigenvalues for the scalar field perturbation were all positive and for the gauge field perturbations they were zero. This was established for a large range of the parameters λ_1, λ_2 and v and we concluded that the configuration was stable, verifying this by a time evolution of the fields. We concluded our work by adding five dimensional gravity to this $U(1) \otimes U(1)$ model and found that this dramatically changes the static gauge field behaviour – there are no longer any non-trivial solutions with sensible boundary conditions.

It would be of interest to investigate further the possibility of full localisation of gauge fields in the $U(1) \otimes U(1)$ model. One would also like to include gravity and a warped metric, but perhaps in a more sophisticated way that allows static gauge field solutions. These two ideas might turn out to augment one another and both should be consider central in future work.

[10]The form $f'' = S(x)f$ with $S(x) \geq 0$ can be thought of as the equation of motion for a mass being pushed away from the origin, as has been noted by many; see pages 17–18 of [14].

A Numerical techniques

Throughout this thesis we constantly come across differential equations which cannot be solved using current analytic methods and we thus revert to numerical (computational) methods. In this section we discuss the three techniques that are be used: finding eigenvalues and associated eigenfunctions; solving second order coupled non-linear ordinary differential equations; and thirdly, time evolving solutions to these ODEs. All these methods are based on the simple idea of discretising the functions we are solving for and approximating their derivatives.

Given a function $f(x)$, we approximate it by considering only those values of the function with x an integral multiple of a small constant h, called the step size. The assumption is that the step size is small enough so $f(x)$ is almost linear between any two adjacent approximation points. The discrete set of values which make up this approximation is denoted $\{f_i\}$ where the index i is an integer corresponding to the integral multiple. We reconstruct the original function by linear interpolation between the points given by

$$f(x = hi) = f_i. \tag{A.1}$$

For functions with an infinite domain, the set $\{f_i\}$ is infinite and not usable in a computational algorithm. We are therefore forced to introduce an artificial "infinity" for x, giving a symmetrical lower and upper bound on i which we denote by $-N$ and N respectively. The number of elements in our discretisation set is then $2N + 1$.

Derivatives of a function approximated as described above can be obtained by Taylor expanding $f(x \pm h)$ as (prime denotes derivative with respect to x)

$$f(h \pm h) = f(x) \pm hf'(x) + \tfrac{1}{2}h^2 f''(x) + O(h^3),$$

and then subtracting or adding these two equations to get, respectively,

$$\begin{aligned} f(x + h) - f(x - h) &= 2hf'(x) + O(h^3), \\ f(x + h) + f(x - h) &= 2f(x) + h^2 f''(x) + O(h^3). \end{aligned}$$

These can be re-arranged and substitutions made for the approximating points to give

$$f'(x) = \tfrac{1}{2h}\left(f_{i+1} - f_{i-1}\right), \tag{A.2}$$

$$f''(x) = \tfrac{1}{h^2}\left(f_{i+1} - 2f_i + f_{i-1}\right), \tag{A.3}$$

which are correct to second order in h, the small step size. This discretisation method and the associated derivative approximations are used extensively in the numerical work that follows.

A.1 Eigensystems

Eigenvalues and their corresponding eigenfunctions (or eigenvectors) are ubiquitous in studies of physical systems. The form that we encounter is reminiscent of finding the energies associated with a known potential in the Schrödinger equation

$$\left(-\tfrac{\mathrm{d}^2}{\mathrm{d}x^2} + S(x)\right) f(x) = \lambda f(x), \tag{A.4}$$

where $f(x)$ is the function to solve for, $S(x)$ is a known, smooth function of the independent variable x and λ is the eigenvalue. We must note that in the cases we encounter, the domain of x is the real line. By applying the approximations given by (A.1) and (A.3), the *differential* equation (A.4) becomes an infinite set of *difference* equations

$$-\tfrac{1}{h^2}\left(f_{i+1} - 2f_i + f_{i-1}\right) + S_i f_i = \lambda f_i. \tag{A.5}$$

To proceed, this set must be truncated to a finite number of equations by introducing a bound for x and i as described previously. Equation (A.5) can then be written as a $2N+1$ dimensional matrix equation

$$\begin{pmatrix} \frac{2}{h^2}+S_{-N} & \dots & 0 & 0 & 0 & \dots & 0 \\ \vdots & \ddots & \vdots & \vdots & \vdots & \ddots & \vdots \\ 0 & \dots & \frac{2}{h^2}+S_{-1} & \frac{-1}{h^2} & 0 & \dots & 0 \\ 0 & \dots & \frac{-1}{h^2} & \frac{2}{h^2}+S_0 & \frac{-1}{h^2} & \dots & 0 \\ 0 & \dots & 0 & \frac{-1}{h^2} & \frac{2}{h^2}+S_1 & \dots & 0 \\ \vdots & \ddots & \vdots & \vdots & \vdots & \ddots & \vdots \\ 0 & \dots & 0 & 0 & 0 & \dots & \frac{2}{h^2}+S_N \end{pmatrix} \begin{pmatrix} f_{-N} \\ \vdots \\ f_{-1} \\ f_0 \\ f_1 \\ \vdots \\ f_N \end{pmatrix} = \lambda \begin{pmatrix} f_{-N} \\ \vdots \\ f_{-1} \\ f_0 \\ f_1 \\ \vdots \\ f_N \end{pmatrix}.$$

Finding the eigenvalues λ and eigenvectors (f_i) of this matrix equation gives a good approximation to the solution of (A.4). Systematic improvements to the approximation should be able to be obtained by decreasing the step size h and increasing the cutoff N. This method should be used to verify the validity of the approximate numerical solution. We note that the matrix is tridiagonal and symmetric and can thus use the `tqli` routine in Numerical Recipes in C [18].

A.2 Ordinary differential equations

The equations we deal with, the field equations of motion, are obtained by finding extrema of an action integral. Akin to Newton's second law, these types of equations are second order differential equations and those which we encounter are (luckily) linear in the second derivative. When there is more than one field, or there is a complex valued field, the equations are generally coupled. To keep things tangible, we initially look for solutions which depend only on one of the independent variables. Thus we are faced with solving second order, linear in the second derivative, not necessarily linear in the first or zeroth derivative, coupled ordinary differential equations. The general form of these types of equations can be written as

$$\frac{\mathrm{d}^2}{\mathrm{d}x^2} f^a(x) = T\left(f^a(x), \tfrac{\mathrm{d}}{\mathrm{d}x} f^a(x)\right), \tag{A.6}$$

where the index a runs over the fields $f^a(x)$ and T is an arbitrary function[11]. The physics will impose boundary conditions on the $f^a(x)$ or its derivatives (or both) as $x \to \pm\infty$. Since the second derivative is linear and there are boundary conditions (as opposed to initial conditions), the relaxation technique for ODEs will be a good way of finding solutions. This entails discretising the $f^a(x)$ as

[11] Note that T does not depend explicitly on the independent variable x because the underlying physics is translationally invariant.

before and making approximations to the derivatives as per (A.2) and (A.3). After some simple algebra, equation (A.6) becomes

$$f_i^a = \tfrac{1}{2}\left(f_{i+1}^a + f_{i-1}^a - h^2 T_i\right), \tag{A.7}$$

where $f_i^a = f^a(hi)$ is again a discretised approximation to the function we are solving for and T_i is the original arbitrary function evaluated at $x = hi$. Note that we use (A.2) to evaluate the first derivative of $f^a(x)$ in the subsequent evaluation of T_i.

Equation (A.7) is an implicit formula for f_i^a given f_{i+1}^a and f_{i-1}^a. It is implicit because T_i can depend on f_i^a and iteration is therefore required to find a solution. This iteration is performed at each i assuming the values to the left and right of f_i^a are correct. One relaxation sweep is completed when all values of i have been visited and the boundary conditions have been imposed. These relaxation sweeps are repeated many times for each field (indexed by a) until the change in the f_i^a between sweeps is sufficiently small. The final approximation must be verified by choosing smaller values for the step size and larger values for the domain cutoff.

A.3 Time evolution

The main aim of this thesis is to establish stability or instability of static field solutions. While the previous two numerical techniques are enough to solve this problem, it is instructive to also visualise the temporal evolution of the equations. Watching a stable solution oscillate or an unstable one collapse, develops our intuition as to what conditions are amenable to a stable solution. Due to the nature of the differential equations (non-linear, coupled, partial and second order), this is a non-trivial exercise and we only rely on the results in a qualitative way.

We make a small generalisation of Section A.2 by allowing our fields to vary in the one time dimension as well as one space dimension, extending equation (A.6) to

$$\left(\frac{\partial^2}{\partial x^2} - \frac{\partial^2}{\partial t^2}\right) f^a(x,t) = T\left(f^a(x,t), \tfrac{\partial}{\partial x} f^a(x,t)\right).$$

We introduce k as a small time step taking us from $f^a(x,t)$ to $f^a(x,t+k)$. Applying the approximations for the derivatives as before and re-arranging, we get

$$f_{i,j+1}^a = 2f_{i,j}^a - f_{i,j-1}^a + \tfrac{k^2}{h^2}\left(f_{i+1,j}^a - 2f_{i,j}^a + f_{i-1,j}^a - h^2 T_{i,j}\right), \tag{A.8}$$

where j is the time index (as opposed to the space index i) and $f_{i,j}^a$ and $T_{i,j}$ are the original functions evaluated at $x = hi$ and $t = kj$. Unlike before, equation (A.8) is an explicit formula for the next time step, making it simple to implement. Given initial conditions for all space at two adjacent times, the complete time evolution can be computed. No attempt is made to prove that this technique is numerically stable and the results obtained are only to be viewed qualitatively. Simple checks on the results are made by decreasing the step sizes, h and k, as before. It is also wise to check that a stable solution computed by the technique in Section A.2 remains the same under the time evolution of (A.8).

Acknowledgements

I would like to thank the following people for ideas, guidance, discussion and keeping me sane: my supervisor Raymond Volkas; members of the group – Alison Demaria, Sandy Law and Catherine Low; those in my office, Jared Cole and Vincent Conrad; also J. Paul Goldby.

I must also thank the wonderful world of free software and those that support it. Specifically the programs that made most of this work possible: Linux for a place to work in; `vim` and `emacs` for editing; `gcc` for compiling my programs; `gnuplot` for plotting my graphs; and LaTeX and friends for typesetting this document.

References

[1] J.S. Rozowsky, R.R. Volkas, and K.C. Wali. Domain wall solutions with abelian gauge fields. *Phys. Lett. B*, 580:249–256, 2004.

[2] L. Randall and R. Sundrum. A large mass hierarchy from a small extra dimension. *Phys. Rev. Lett*, 83:3370–3373, 1999. hep-ph/9905221.

[3] L. Randall and R. Sundrum. An alternative to compactification. *Phys. Rev. Lett.*, 83:4690–4693, 1999. hep-th/9906064.

[4] H.C. Lee, editor. *An Introduction to Kaluza-Klein Theories*, pages 1–9. World Scientific Publishing Co. Pte. Ltd., 1984. English translation by T. Muta of Th. Kaluza's *On the Unification Problem in Physics*.

[5] H.C. Lee, editor. *An Introduction to Kaluza-Klein Theories*, pages 10–22. World Scientific Publishing Co. Pte. Ltd., 1984. English translation by T. Muta of O. Klein's *Quantum Theory and Five-Dimensional Relativity*.

[6] N. Arkani-Hamed, S. Dimopoulos, and G.R. Dvali. The hierarchy problem and new dimensions at a millimeter. *Phys. Lett. B*, 429:263, 1998. hep-ph/9803315.

[7] I. Antoniadis, N. Arkani-Hamed, S. Dimopoulos, and G.R. Dvali. New dimensions at a millimeter to a fermi and superstrings at a tev. *Phys. Lett. B*, 436:257, 1998. hep-ph/9804398.

[8] N. Arkani-Hamed, S. Dimopoulos, and G.R. Dvali. Phenomenology, astrophysics and cosmology of theories with sub-millimeter dimensions and tev scale quantum gravity. *Phys. Rev. D*, 59(086004), 1999. hep-ph/9807344.

[9] C. Ringeval, P. Peter, and J.P. Uzan. Localization of massive fermions on the brane. *Phys. Rev. D*, 65(044016), 2002.

[10] A. Davidson and P.D. Mannheim. Dynamical localization of gravity. hep-th/0009064, 2000.

[11] G. Dvali and M. Shifman. Domain walls in strongly coupled theories. *Phys. Lett. B*, 396:64–69, 1997. hep-th/9612128.

[12] S.L. Dubovsky and V.A. Rubakov. On models of gauge field localization on a brane. *Int. J. Mod. Phys. A*, 16:4331–4350, 2001. hep-ph/0105243.

[13] M.J. Duff. Kaluza-klein theory in perspective. In *Proceedings of the Symposium, The Oskar Klein Centenary. World Scientific. Singapore*, pages 22–35, 1995. hep-th/9410046.

[14] R. Rajaraman. *Solitons and instantons : an introduction to solitons and instantons in quantum field theory*. North-Holland Pub. Co., 1982.

[15] D. Bazeia, C. Furtado, and A.R. Gomes. Brane structure from a scalar field in warped spacetime. *J. Cosmol. Astropart. Phys.*, JCAP02(002), 2004. hep-th/0308034.

[16] A. Davidson, B.F. Toner, R.R. Volkas, and K.C. Wali. Clash of symmetries on the brane. *Phys. Rev. D*, 65(125013), 2002. hep-th/0202042.

[17] G. Dando, A. Davidson, R.R. Volkas, and K.C. Wali. The clash of symmetries in a randall-sundrum-like spacetime. Manuscript in preparation.

[18] William H. Press, Saul A. Teukolsky, William T. Vetterling, and Brian P. Flannery. *Numerical Recipes in C: The Art of Scientific Computing*. Cambridge University Press, 1992.